Heliyon 10 (2024) e40481

Contents lists available at ScienceDirect

Heliyon

journal homepage: www.cell.com/heliyon

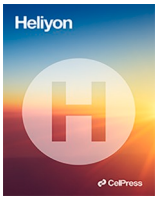

Research article

Advancing analytical and graphical methods for binary and ternary mixtures: The toxic interactions of divalent metal ions in human lung cells

James Y. Liu [a], Jonathan M. Beard [a], Saber Hussain [b], Christie M. Sayes [a,*]

[a] Department of Environmental Science, Baylor University, Waco, TX 76798-7266, USA
[b] 711th Human Performance Wing, Air Force Research Laboratory, Dayton, OH, USA

ARTICLE INFO

Keywords:
Toxicology
Mixtures
Interactions
Isobologram
Regression
Modeling

ABSTRACT

Humans are exposed to various environmental chemicals, particles, and pathogens that can cause adverse health outcomes. These exposures are rarely homogenous but rather complex mixtures in which the components may interact, such as through synergism or antagonism. Toxicologists have conducted preliminary investigations into binary mixtures of two components, but little work has been done to understand mixtures of three or more components. We investigated mixtures of divalent metal ions, quantifying the toxic interactions in a human lung model. Eight metals were chosen: heavy metals cadmium, copper, lead, and tin, as well as transition metals iron, manganese, nickel, and zinc. Human alveolar epithelial cells (A549) were exposed to individual metals and sixteen binary and six ternary combinations. The dose-response was modeled using logistic regression in R to extract LC_{50} values. Among the individual metals, the highest and lowest toxicity were observed with copper at an LC_{50} of 102 μM and lead at an LC_{50} of 5639 μM, respectively. First and second-order interaction coefficients were obtained using machine learning-based linear regression in Python. The resulting second-degree polynomial model formed either a hyperbolic or elliptical conic section, and the positive quadrant was used to produce isobolograms and contour plots. The strongest synergism and antagonism were observed in cadmium-copper and iron-zinc, respectively. A three-way interaction term was added to produce full ternary isobologram surfaces, which, to our knowledge, are a significant first in the toxicology literature.

1. Introduction

Humans are exposed to a variety of toxicants in the environment, including through inhalation. This exposure route is of particular concern in the occupational setting, where workers are repeatedly exposed to higher-than-normal concentrations of aerosolized substances such as minerals, metals, exhaust fumes, and organics [1,2]. The field of toxicology aims to achieve a thorough understanding of these exposures, including the mechanisms of toxic action and the overall risks involved. Because humans are often exposed to a complex mixture of toxicants rather than singular chemicals or particles, understanding the toxic interactions in mixtures remains a major enduring challenge for the field [3,4].

* Corresponding author. Department of Environmental Science, Baylor University, One Bear Place #97266, Waco, TX 76798-7266, USA.
E-mail address: Christie_sayes@baylor.edu (C.M. Sayes).

https://doi.org/10.1016/j.heliyon.2024.e40481
Received 25 April 2024; Received in revised form 14 November 2024; Accepted 14 November 2024
Available online 16 November 2024

Traditionally, mixture interactions have been analyzed under concentration addition and independent action frameworks [5]. Concentration addition is the most common assumption, which presumes that toxicants have a similar mode of action such that any quantity of a toxicant could be replaced with the equivalent quantity of another. Independent action instead proposes that toxicants have dissimilar modes of action. Calculated values, such as toxic units and toxicity indices, have been applied to approximate the overall potency of a mixture or its broader characteristics, typically the presence of synergism or antagonism [6,7].

Several graphical methods have also been developed for binary mixtures, with isobolograms being the most used. In two dimensions, an isobologram contains axes corresponding to the two components and a curve representing all mixture ratios that produce a biological effect at a given threshold [8–10]. This is typically a set of EC_{50} or LC_{50} values equivalent to a contour of the three-dimensional response surface [11–13]. Isobolograms often include a line of additivity connecting the two intercepts (*e.g.,* individual component EC_{50} values). If the curve falls below or above the additive line, the behavior is considered synergistic or antagonistic, respectively.

Most of the theory behind mixtures toxicology is borrowed from or co-developed with concepts from pharmacology [14]. Most commonly, the pharmaceutical industry is concerned with undesired interference between two drugs a patient may take and the design of synergistic treatments [13,15]. The motivations impact toxicology, where there are few tools for analyzing mixtures of more than two components [16,17]. Because higher-order mixtures have exponentially more possible combinations, the potential resources required also serve as a deterrent [18]. We aim to show that it is possible to delve into ternary mixtures and expand our understanding through innovative techniques, both analytical and graphical.

For this study, we focused on metal ion mixture toxicity in the lungs [19,20]. Four heavy metals (cadmium, copper, lead, and tin) and four transition metals (iron, manganese, nickel, and zinc) were chosen to represent a range of substances where human occupational co-exposures might occur. All eight metals are mined from the earth's crust, with potential inhalation exposure during the mining and extraction. The metals are often present as impurities amongst each other; for example, cadmium may be obtained during the processing of zinc ores [21]. Copper, iron, lead, manganese, nickel, tin, and zinc are all commonly used in alloys, leading to workers' potential inhalation of mixed particles during their production or the subsequent manufacture of parts [22,23]. There are also other shared applications, such as batteries, ceramics, electronics, paints, and welding [24,25]. Once metal particles deposit in the lungs, ions are released, especially if they are compartmentalized into the acidic environment of macrophages [26]. Prior studies have shown the presence of divalent ions of cadmium, copper, iron, manganese, nickel, zinc, and other metals in the lungs, as well as potential mechanisms behind some of their interactions [27–30]. While the speciation of individual metals may vary, the focus on divalent ions in this study is to increase the probability of observing interactions due to related mechanisms of action.

Using a medium-throughput approach, we quantified binary and ternary mixture interactions for toxicity of the eight metal ions toward human lung cells. These interactions were visualized using isobolograms and response surfaces. To our knowledge, the three-dimensional ternary isobolograms are the first in the toxicology literature [31].

2. Materials and methods

Materials. All chemicals and supplies - cadmium chloride, copper chloride, iron chloride, lead nitrate, manganese chloride, nickel chloride, tin chloride, zinc chloride, cell culture supplies, and CellTiter 96AQ One Solution Cell Proliferation (MTS) assay - were obtained from Fisher Scientific (Waltham, MA, USA). A549 human alveolar epithelial cells (Catalog number: CCL-185 and RRID: CVCL_0023) were obtained from ATCC (Manassas, VA, USA). Prior to initial use, cells were authenticated via STR analysis and tested for mycoplasma contamination via Hoechst DNA stain, agar culture, and PCR-based assay (none detected).

Metal ion cytotoxicity. A549 cells (passages 14–24) were cultured at 37 °C and 5 % CO_2 using RPMI 1640 media supplemented with 10 % fetal bovine serum and 1 % penicillin-streptomycin solution (5000 U/mL). After reaching 95 % confluency, cells were plated at 10,000 cells per well on 96-well plates and incubated 24 h before exposure. All chemicals were dissolved in fresh media and bath sonicated for 15 min. Each well was dosed by replacing the media with 200 μL of metal ion solution. A 0.1 % v/v Triton X-100 solution was used as a positive control for cell death, and an untreated control was used. Exposed cells were incubated for 24 h before adding 1:5 MTS:media. Cells were then incubated for 2 h before 490 nm absorbance reading on a Biotek H1 Synergy plate reader obtained from Agilent (Santa Clara, CA, USA). All data are an average of four replicates.

Mixtures interactions model. For a mixture of k components and a given response (*e.g.,* a biological endpoint, such as live/dead), the response space has k+1 dimensions. A set response level results in k-dimensional iso-contours. For example, the response surface is three-dimensional in a binary mixture (k = 2), and the iso-contours at R = 0, R = 0.5, R = 1, etc., are two-dimensional. Assuming concentration addition yields purely additive behavior in a straight line, described by **Equation (1)** for binary mixtures and adding only a two-way interaction term results in hyperbolic behavior, as described by **Equation (2)**. However, self-interactions are also possible for a 2nd-degree polynomial model, resulting in **Equation (3)**.

$$b_1x_1 + b_2x_2 - 1 = 0 \tag{1}$$

$$b_{12}x_1x_2 + b_1x_1 + b_2x_2 - 1 = 0 \tag{2}$$

$$b_{11}{x_1}^2 + b_{12}x_1x_2 + b_{22}{x_2}^2 + b_1x_1 + b_2x_2 - 1 = 0 \tag{3}$$

Extending this model to ternary mixtures (k = 3), the additive behavior results in a plane instead of a line, as described by **Equation (4)**. The iso-contour is now a surface with curvature. Among the ten possible third-order terms, we only included the three-way interaction term to avoid overfitting to limited data and overcomplicating the analyses. This model is described by **Equation (5)**.

$$b_1x_1 + b_2x_2 + b_3x_3 - 1 = 0 \quad (4)$$

$$b_{123}x_1x_2x_3 + b_{11}{x_1}^2 + b_{22}{x_2}^2 + b_{33}{x_3}^2 + b_{12}x_1x_2 + b_{13}x_1x_3 + b_{23}x_2x_3 + b_1x_1 + b_2x_2 + b_3x_3 - 1 = 0 \quad (5)$$

Modeling and statistics. Dose-response curves and LC_{50} values for all exposures were modeled in R using logistic regression from a binomial generalized linear model (GLM). To obtain all first and second-order interaction coefficients, machine learning linear regression was conducted using numpy and scikit-learn packages in Python. Data were then processed to generate binary/ternary isobolograms and contour plots using the ggpubr, orca, plotly, tidyverse, and viridis packages in R [32–36].

3. Results and Discussion

Exposures were conducted for individual, binary, and ternary combinations in sequence, with concentrations and mixing ratios chosen to maximize information gain at each step. Although this study did not explore every possible mixture combination, each evaluated combination represents a plausible co-exposure scenario due to shared commercial and industrial applications for the component metals.

The dose-response curves for the eight individual metal ions were presented in Fig. 1. Each point averages four replicates, while simple logistic regression was used to model the curve. The LC_{50} values in Table 1, representing the concentration of a toxicant that causes 50 % cell death, were calculated from the model coefficients. The dose-response curves and LC_{50} values for mixtures were calculated similarly and can be found in the supplemental information (Fig. S1 and Table S1). Among the individual divalent metal ions, copper was the most toxic, with an LC_{50} of 102 μM, while lead was the least toxic, with an LC_{50} of 5639 μM. The ranked individual toxicities align strongly with a prior study for Cu, Fe, Mn, and Zn [37]. The only exception is Pb, a discrepancy that may warrant future investigation.

Sixteen binary combinations of metal ions were tested for cytotoxicity to determine both self-interactions (*e.g.,* Cd is the basic linear effect of cadmium while Cd:Cd is cadmium interacting with itself) and mixed interactions (*e.g.,* Fe:Mn is the interaction between Fe and Mn). These interactions can be caused by parallel action, competition for receptors, or other mechanisms along the toxicity pathway. The resulting isobolograms and contour plots for binary mixtures are shown in Figs. 2 and 3, respectively. The solid gray lines represent strictly additive behavior (**Equation (1)**) with no 2nd order interaction terms. The dashed colored lines show the isobologram as obtained from modeling experimental data. **Equation (2)** represents a simple hyperbolic model without self-interaction terms for each component, while **Equation (3)** represents the full second-degree polynomial model used in this study, which is also the general form for a conic section.

Compared to the simple hyperbolic model, the full second-degree model allows for both hyperbolic and elliptical behavior [38–40]. The full model can better capture strongly antagonistic behavior, as seen with Cu:Ni, Fe:Zn, and Zn:Cd. When using the simple model, the extreme points for Cu:Ni and Zn:Cd cause the hyperbolic to become unstable and inverted, while the extreme point for Fe:Zn causes a false reflection to the lower branch (Fig. S2). The full model does not encounter these difficulties, and additional self-interaction terms present constraints that result in higher consistency across the data.

A summary of the binary mixture results is reported in Table 2. Amongst the 16 binary combinations, seven were hyperbolic, and nine were elliptical. Regarding overall interaction, five were synergistic, five were additive, and six were antagonistic. The strongest synergism was observed in Cd:Cu, while the strongest antagonism was observed in Fe:Zn. With a set of only eight similar toxicants, the

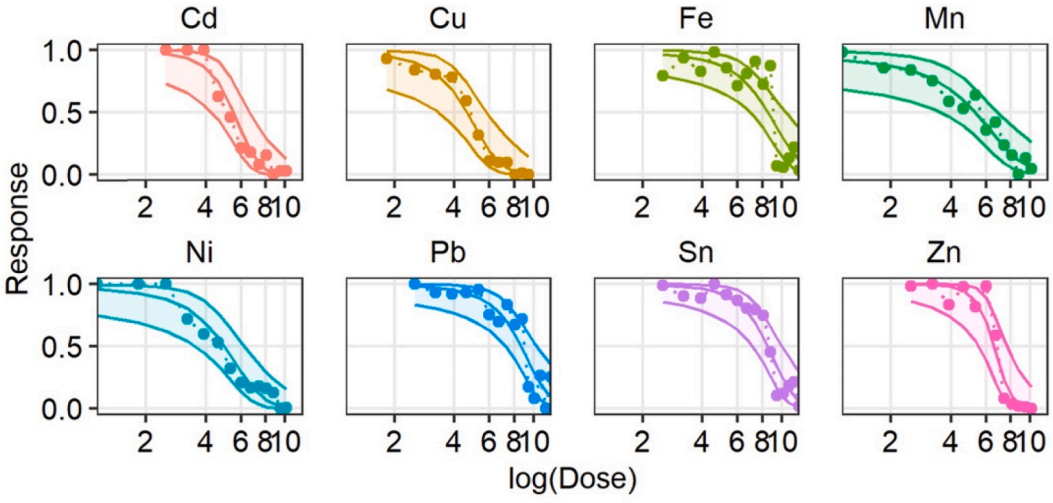

Fig. 1. Dose-response curves for the cytotoxicity of individual metal ions to A549 cells. The dose in μM is reported on a log axis (3.125 μM–204800 μM), while the response ranges from 0 to 1 (0 %–100 % viable cells). Metals include cadmium (Cd), copper (Cu), iron (Fe), manganese (Mn), nickel (Ni), lead (Pb), tin (Sn), and zinc (Zn). The coordinates for all plots are identical.

Table 1
LC_{50} values in μM for all individual metal ion exposures as determined by logistic regression.

Metal Ion	LC_{50} (μM)
Cd^{2+}	236
Cu^{2+}	102
Fe^{2+}	4850
Mn^{2+}	192
Ni^{2+}	138
Pb^{2+}	5639
Sn^{2+}	4764
Zn^{2+}	701

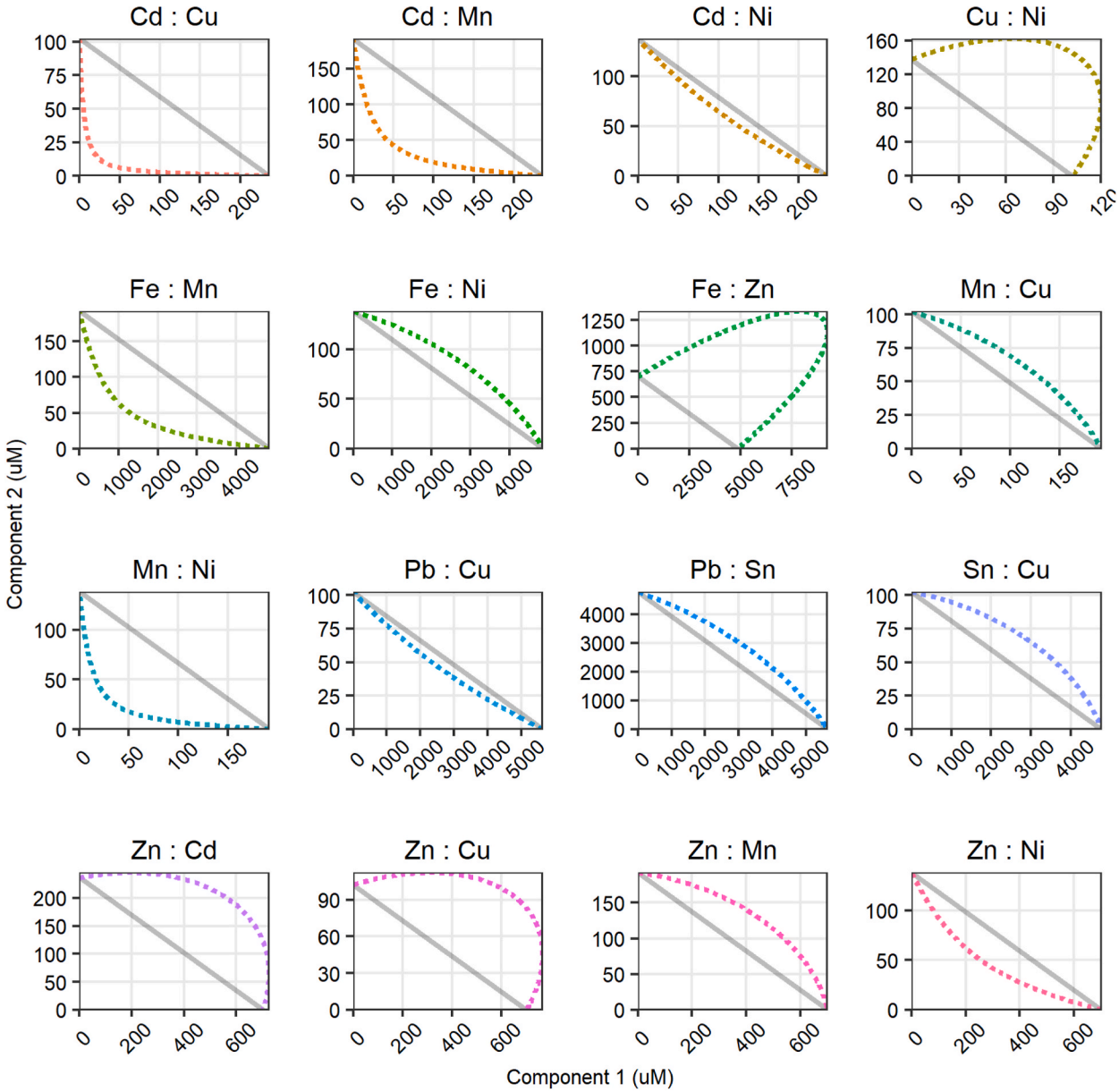

Fig. 2. Binary mixture isobolograms for all tested combinations. Solid gray lines represent a theoretical additive relationship, while dashed colored lines show the observed behavior. Panels are labeled as [Component 1: Component 2]. The model used is described by **Equation (3)**.

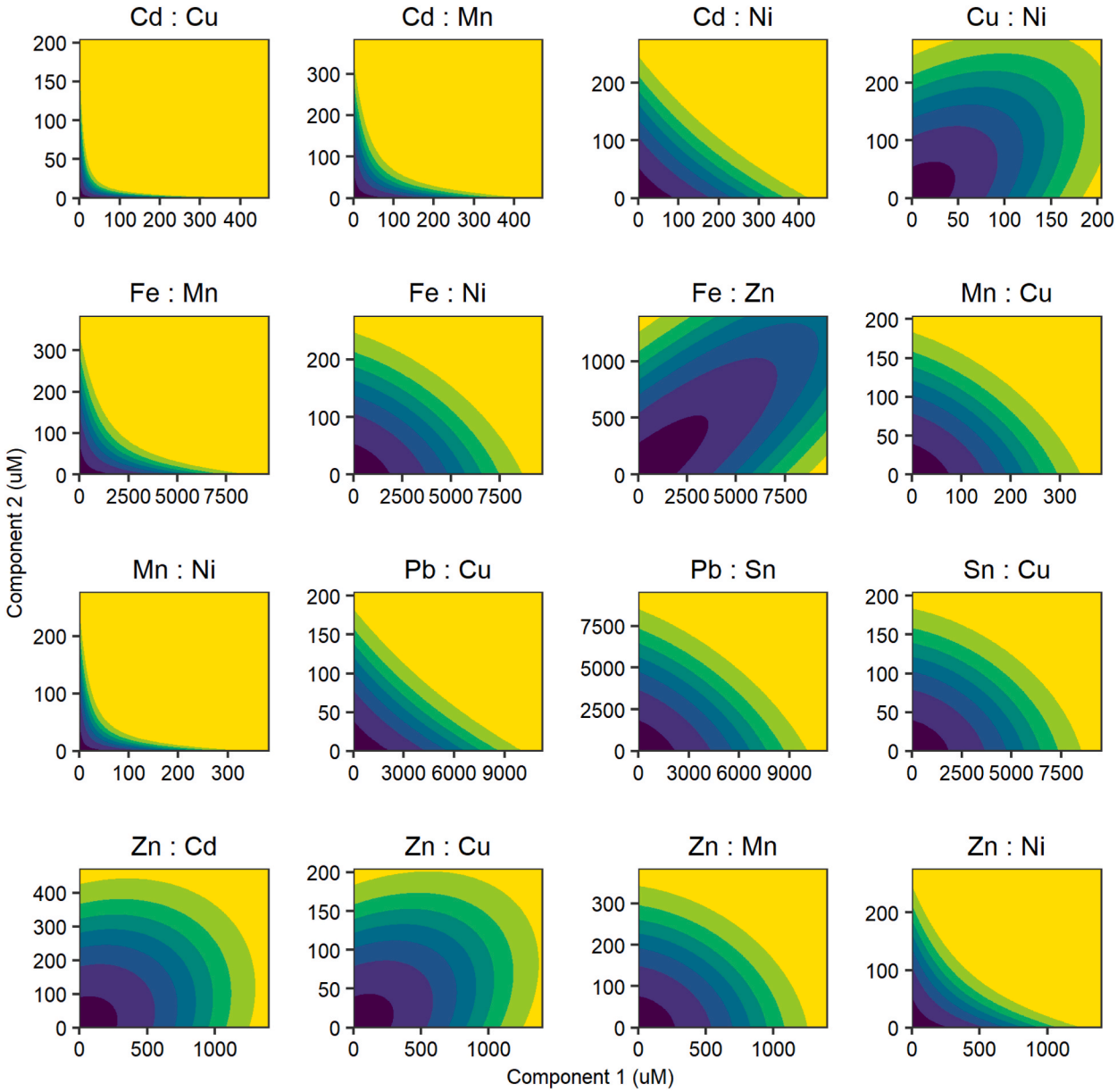

Fig. 3. Binary mixture contour plots showing an estimated response gradient. The darker region represents low cytotoxicity, while the brighter region represents high cytotoxicity. Panels are labeled as [Component 1: Component 2]. The model used is described by **Equation (3)**.

full range of interaction modes was observed. Previous studies on metal ion mixtures toxicity in lung cells are rare, though there are adjacent studies that may use related toxicants (*e.g.*, metal oxide nanoparticles) or animal models [37,41,42]. Within this narrow range of potentially comparable results, there is mixed agreement (*e.g.*, the Fe:Mn interaction is found to be synergistic in Yuan et al. but antagonistic in Wang et al., compared to the synergism reported here). The richness of mixture interactions found here emphasizes the continued need to expand our understanding of how toxicants can combine and produce novel toxic effects.

Six ternary combinations of metal ions were tested to capture different behaviors and potential co-exposure scenarios. The resulting LC_{50} values and previously determined 1st and 2nd order terms were used to calculate three-way interaction coefficients. These were then used to plot ternary isobolograms, shown in Fig. 4. The grayscale triangles are planes of additivity (**Equation (4)**), while the colored surfaces are the ternary isobolograms (**Equation (5)**). While there are ten possible 3rd order interaction terms (*e.g.*, $x_1^2x_2$ and x_1^3), we chose only to include the three-way term (x_1:x_2:x_3) to avoid overfitting the limited data and overcomplicating the analyses.

The ternary Zn:Mn:Cu was found to be synergistic, though this only had the effect of dampening the overall antagonism from the binary interactions. The ternary Pb:Sn:Cu was additive, and the remainder were antagonistic. The overall interaction behavior of the mixture (account for both binary and ternary interactions) can be identified as synergistic or antagonistic when a given point on the

Table 2
Summary of overall results for binary mixtures. The shape of the conic section is either hyperbolic (H) or elliptical (E) as determined by the discriminant. The resulting interaction is labeled as synergistic (S), additive (–), or antagonistic (A).

Mixture	Shape	Result
Cd: Cu	H	S
Cd: Mn	H	S
Cd: Ni	H	–
Cu: Ni	E	A
Fe: Mn	H	S
Fe: Ni	E	–
Fe: Zn	E	A
Mn: Cu	E	–
Mn: Ni	H	S
Pb: Cu	H	–
Pb: Sn	E	–
Sn: Cu	E	A
Zn: Cd	E	A
Zn: Cu	E	A
Zn: Mn	E	A
Zn: Ni	H	S

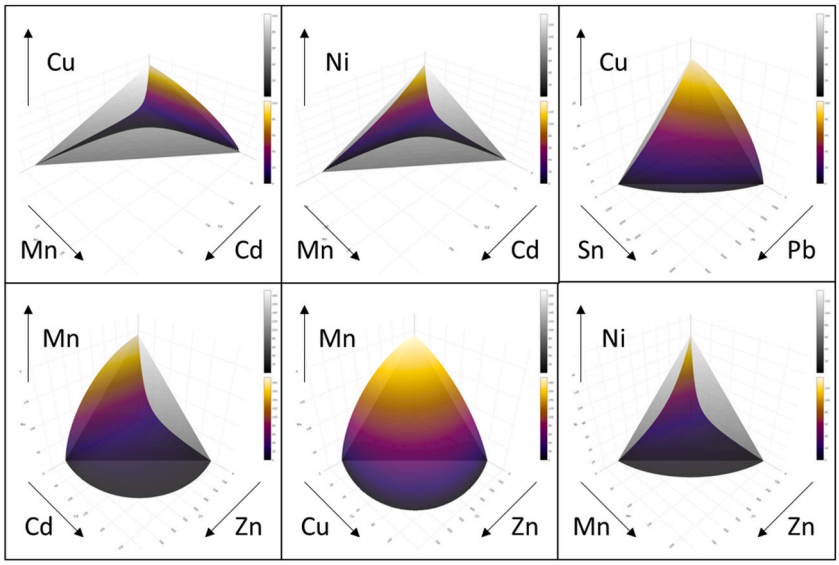

Fig. 4. Ternary mixture isobolograms for all tested combinations. Grayscale triangular planes represent theoretical additive relationships. Colored surfaces represent the observed behavior. Axes were re-labeled for visibility. The model used is described by **Equation (5)**.

surface falls below or above the plane of additivity, respectively.

We have not seen any ternary isobolograms in the toxicology literature, and only four examples in the pharmacology literature. Of those, three present a scatter of points, while only one shows a mesh isobologram surface [43–46]. Here, we not only generated fully-resolved surfaces but could do so for multiple combinations effectively. We also quantified the underlying interactions using our model, whereas the existing studies only present averaged or single-point index values. Visualizing the entire surface is important because the isobologram can cross the plane of additivity in three dimensions, indicating an inflection in overall behavior that is important to consider when estimating risk [4].

4. Conclusions

Advancing our understanding of mixtures has been a persistent challenge in toxicology and human health risk assessment. In this study, we investigated binary and ternary combinations of divalent metal ions that have a wide range of commercial and industrial applications, leading to a variety of mixture exposure scenarios. We used an efficient design to collect data on their toxicity in an *in vitro* human lung model. Using a combination of logistic regression, linear regression, and a mixture interactions model, we generated a large set of fully-resolved 2D and 3D isobolograms. To our knowledge, this is the first such study in the toxicology literature [31].

There are many options to continue along the trajectory of the methods presented here. Expanding the ternary data with additional points would help improve estimates for the interaction terms. This would also allow the computation of ternary isobolograms using all 3rd order terms, possibly even with nonlinear terms [47]. Such an implementation might utilize the marching cubes algorithm or similar methods for estimating 3D contours from 4D data [48]. Other future work could involve expanding to more diverse combinations of toxicants that are still suspected to act along similar pathways, exploring new biological models or endpoints, or introducing heterogenous factors such as environmental conditions. As high-throughput experimental designs continue to progress, it may even be feasible to develop sophisticated models for quaternary mixtures or beyond. Sufficiently thorough screening could also pave the way for predicting interactions across classes of toxicants.

CRediT authorship contribution statement

James Y. Liu: Writing – original draft, Visualization, Validation, Software, Methodology, Investigation, Formal analysis, Data curation. **Jonathan M. Beard:** Writing – original draft, Methodology, Investigation, Formal analysis, Data curation. **Saber Hussain:** Resources, Project administration, Funding acquisition. **Christie M. Sayes:** Writing – review & editing, Writing – original draft, Visualization, Validation, Supervision, Software, Resources, Project administration, Methodology, Investigation, Funding acquisition, Formal analysis, Data curation, Conceptualization.

Data availability statement

Data will be made available on request.

Declaration of competing interest

The authors declare that they have no known competing financial interests or personal relationships that could have appeared to influence the work reported in this paper.

Acknowledgments

JYL received student internship funds from the Oak Ridge Institute for Science and Education (ORISE) through an interagency agreement between the U.S. Department of Energy and the Air Force Research Laboratory (AFRL-2023-4907). JYL, JB, and CMS thank the Baylor Department of Environmental Science and the Henry M Jackson Foundation xfor financially supporting this research.

Appendix A. Supplementary data

Supplementary data to this article can be found online at https://doi.org/10.1016/j.heliyon.2024.e40481.

References

[1] P. Cullinan, et al., Occupational lung diseases: from old and novel exposures to effective preventive strategies, Lancet Respir. Med. 5 (5) (2017) 445–455.
[2] J.Y. Liu, C.M. Sayes, A toxicological profile of silica nanoparticles, Toxicol. Res. 11 (4) (2022) 565–582.
[3] R. Altenburger, M. Nendza, G. Schuurmann, Mixture toxicity and its modeling by quantitative structure-activity relationships, Environ. Toxicol. Chem. 22 (8) (2003) 1900–1915.
[4] M. Sigurnjak Bureš, et al., Modeling the toxicity of pollutants mixtures for risk assessment: a review, Environ. Chem. Lett. 19 (2) (2021) 1629–1655.
[5] Y. Liu, et al., Toxicity models of metal mixtures established on the basis of "additivity" and "interactions", Front. Environ. Sci. Eng. 11 (2) (2017).
[6] J.B. Belden, The acute toxicity of pesticide mixtures to honeybees, Integr Environ Assess Manag 18 (6) (2022) 1694–1704.
[7] Q. Liu, et al., Prioritization of micropollutants in municipal wastewater and the joint inhibitory effects of priority organic pollutants on Vibrio qinghaiensis sp.-Q67, Aquat. Toxicol. 252 (2022) 106288.
[8] R.Y. Huang, et al., Isobologram analysis: a comprehensive review of methodology and current research, Front. Pharmacol. 10 (2019) 1222.
[9] C. Collom, et al., Toxicity of binary mixtures of copper, lead, and glyphosate on neuronal cells, Journal of Hazardous Materials Advances 11 (2023).
[10] Y. Baldovinos, et al., Chemical interactions and cytotoxicity of terpene and diluent vaping ingredients, Chem. Res. Toxicol. 36 (4) (2023) 589–597.
[11] H. Toumi, et al., Combined acute ecotoxicity of malathion and deltamethrin to Daphnia magna (Crustacea, Cladocera): comparison of different data analysis approaches, Environ. Sci. Pollut. Res. Int. 25 (18) (2018) 17781–17788.
[12] L. Xing, et al., Combined toxicity of three chlorophenols 2,4-dichlorophenol, 2,4,6-trichlorophenol and pentachlorophenol to Daphnia magna, J. Environ. Monit. 14 (6) (2012) 1677–1683.
[13] J. Niu, R.M. Straubinger, D.E. Mager, Pharmacodynamic drug-drug interactions, Clin. Pharmacol. Ther. 105 (6) (2019) 1395–1406.
[14] P.K. Gessner, Isobolographic analysis of interactions: an update on applications and utility, Toxicology 105 (2–3) (1995) 161–179.
[15] A.G. Roberts, M.E. Gibbs, Mechanisms and the clinical relevance of complex drug-drug interactions, Clin. Pharmacol. 10 (2018) 123–134.
[16] J. Foucquier, M. Guedj, Analysis of drug combinations: current methodological landscape, Pharmacol Res Perspect 3 (3) (2015) e00149.
[17] K.A. Ryall, A.C. Tan, Systems biology approaches for advancing the discovery of effective drug combinations, J Cheminform 7 (2015) 7.
[18] O. Martin, et al., Ten years of research on synergisms and antagonisms in chemical mixtures: a systematic review and quantitative reappraisal of mixture studies, Environ. Int. 146 (2021) 106206.
[19] A.V. Menon, J. Chang, J. Kim, Mechanisms of divalent metal toxicity in affective disorders, Toxicology 339 (2016) 58–72.
[20] M.D. Cohen, Pulmonary immunotoxicology of select metals: aluminum, arsenic, cadmium, chromium, copper, manganese, nickel, vanadium, and zinc, J Immunotoxicol 1 (1) (2004) 39–69.
[21] M. Achternbosch, et al., Cadmium flows caused by the worldwide production of primary zinc metal, J. Ind. Ecol. 13 (3) (2009) 438–454.

[22] W. Hume-Rothery, B.R. Coles, The transition metals and their alloys, Adv. Phys. 3 (10) (1954) 149–242.
[23] T.S. Peixe, et al., Occupational exposure profile of Pb, Mn, and Cd in nonferrous Brazilian sanitary alloy foundries, Toxicol. Ind. Health 30 (8) (2014) 701–713.
[24] K.T. Palmer, et al., Inflammatory responses to the occupational inhalation of metal fume, Eur. Respir. J. 27 (2) (2006) 366–373.
[25] O.K. Kurt, N. Basaran, Occupational exposure to metals and solvents: allergy and airway diseases, Curr. Allergy Asthma Rep. 20 (8) (2020) 38.
[26] W.S. Cho, et al., Zeta potential and solubility to toxic ions as mechanisms of lung inflammation caused by metal/metal oxide nanoparticles, Toxicol. Sci. 126 (2) (2012) 469–477.
[27] M. Peana, et al., Metal toxicity and speciation: a review, Curr. Med. Chem. 28 (35) (2021) 7190–7208.
[28] M. Mantha, et al., Fe- and Zn-induced inhibition of Cd uptake in human lung cell lines: speciation studies with H441 and A549 cells, Toxicol. Vitro 25 (8) (2011) 1701–1711.
[29] J. Hedberg, et al., The importance of extracellular speciation and corrosion of copper nanoparticles on lung cell membrane integrity, Colloids Surf. B Biointerfaces 141 (2016) 291–300.
[30] J.E. Goodman, et al., The nickel ion bioavailability model of the carcinogenic potential of nickel-containing substances in the lung, Crit. Rev. Toxicol. 41 (2) (2011) 142–174.
[31] J.Y. Liu, C.M. Sayes, Modeling mixtures interactions in environmental toxicology, Environ. Toxicol. Pharmacol. 106 (2024) 104380.
[32] A. Kassambara, Ggpubr: 'ggplot2' Based Publication Ready Plots, 2023.
[33] C. Sievert, Interactive Web-Based Data Visualization with R, Plotly, and Shiny, 2020.
[34] H. Wickham, et al., Welcome to the tidyverse, J. Open Source Softw. 4 (43) (2019).
[35] S. Garnier, et al., viridis(Lite) - Colorblind-Friendly Color Maps for R, 2023.
[36] T. Hočevar, J. Demčar, Computation of graphlet Orbits for nodes and edges in sparse graphs, J. Stat. Software 71 (10) (2016).
[37] Y. Yuan, et al., In vitro toxicity evaluation of heavy metals in urban air particulate matter on human lung epithelial cells, Sci. Total Environ. 678 (2019) 301–308.
[38] B.A. Katsnelson, et al., Further development of the theory and mathematical description of combined toxicity: an approach to classifying types of action of three-factorial combinations (a case study of manganese-chromium-nickel subchronic intoxication), Toxicology 334 (2015) 33–44.
[39] V.G. Panov, A.N. Varaksin, Identification of combined action types in experiments with two toxicants: a response surface linear model with a cross term, Toxicol. Mech. Methods 26 (2) (2016) 139–150.
[40] A.N. Varaksin, et al., Using various nonlinear response surfaces for mathematical description of the type of combined toxicity, Dose Response 16 (4) (2018) 1559325818816596.
[41] I.A. Minigalieva, et al., In vivo toxicity of copper oxide, lead oxide and zinc oxide nanoparticles acting in different combinations and its attenuation with a complex of innocuous bio-protectors, Toxicology 380 (2017) 72–93.
[42] Y. Wang, et al., Synergistic and antagonistic interactions among organic and metallic components of the ambient particulate matter (PM) for the cytotoxicity measured by Chinese hamster ovary cells, Sci. Total Environ. 736 (2020) 139511.
[43] I. Chumakov, et al., Polytherapy with a combination of three repurposed drugs (PXT3003) down-regulates Pmp 22 over-expression and improves myelination, axonal and functional parameters in models of CMT1A neuropathy, Orphanet J. Rare Dis. 9 (2014) 201.
[44] C. Xiaobo, et al., TUSC2(FUS1)-erlotinib induced vulnerabilities in epidermal growth factor receptor(EGFR) wildtype non-small cell lung cancer(NSCLC) targeted by the repurposed drug auranofin, Sci. Rep. 6 (2016) 35741.
[45] D.E. Kent, et al., Binding site location on GABA(A) receptors determines whether mixtures of intravenous general anaesthetics interact synergistically or additively in vivo, Br. J. Pharmacol. 176 (24) (2019) 4760–4772.
[46] L. Chiaraviglio, J.E. Kirby, High-throughput intracellular antimicrobial susceptibility testing of Legionella pneumophila, Antimicrob. Agents Chemother. 59 (12) (2015) 7517–7529.
[47] G.E. Jarvis, A.J. Thompson, A golden approach to ion channel inhibition, Trends Pharmacol. Sci. 34 (9) (2013) 481–488.
[48] T.S. Newman, H. Yi, A survey of the marching cubes algorithm, Comput. Graph. 30 (5) (2006) 854–879.